RSC Advances




ROYAL SOCIETY OF CHEMISTRY

www.rsc.org/advances

**Submitted to *RSC Advances***

# Fluorinated Silsesquioxane-based Photoresist as Ideal Material with High-Performance for Ultraviolet Nanoimprinting

Guanghui Lin, Fang Zhang, Qi Zhang, Jie Wei,* Jinbao Guo*

College of Materials Science and Engineering, Beijing University of Chemical Technology, Beijing 100029, P. R. China.

* Correspondence to: Jinbao Guo (guojb@mail.buct.edu.cn)

Jie Wei (weij@mail.buct.edu.cn).

**Abstract:**

In this study, we develop a new kind of functional photoresist based on octamethacrylated polyhedral oligomeric silsesquioxane (MAPOSS) and fluorinated monomer as an ideal material for ultraviolet nanoimprint lithography (UV-NIL). We firstly described the optimum synthesis of MAPOSS by the hydrolysis and condensation reactions of methacryloyl oxygen propyl trimethoxysilane, the hybrid photoresist formulations with MAPOSS and fluorinated additive was found to be effective materials for high-performance UV-NIL, which exhibit preferable curing rate, Young's modulus and thermal stability. Additionally, the low shrinkage and low surface energy of the curing film allows easier transfer of relief features with excellent imprint reliability for UV-based NIL techniques. These characteristics of the fluorinated silsesquioxane-based photoresist make them suitable as inexpensive and convenient components in UV-NIL processes.

**Key words:**

Polyhedral oligomeric silsesquioxane, Fluorinated silsesquioxane-based photoresist, low surface energy, UV nanoimprint lithography

## Introduction

Nanoimprint lithography (NIL) technology has attracted enormous attentions in a wide range of areas including high density storage, organic thin-film transistors, photonic crystals, bio-microfluidical, solar cell, sensors and high-precision printed circuit board. Compared with conventional nanofabrication methods, NIL technology has many advantages such as acceptable cost, high resolution and insurmountably micro-replication process. [1-12] Among them, ultraviolet NIL (UV-NIL) is suitable for high-resolution, high-throughput, and low-cost nanofabrication process.[13,14] An ideal UV imprintable resist should have excellent properties such as low enough viscosity, fast photopolymerization with minimal shrinkage, and enough thermal stability.[15] Meanwhile, another concern for UV nanoimprint lithography is the defect caused by adhesion and friction during the separation process, which can cause deformation and breakdown of the transferred patterns on the polymer.[16] As is well known, there exist two main interfaces in NIL process, one is the interface between the mold and the polymer film and another is the interface between the polymer film and the substrate. So long as the surface energy of the materials including photoresist, mold and the substrate is appropriately controlled, the defects from the adhesion strength in the interfaces can be effectively reduced.[17] Therefore, there is a need to design new chemical species that can effectively address to the above two points in a hybrid photoresist system.

Recently, many functional polyhedral oligomeric silsesquioxane (POSS) derivatives have been applied as photoresists or replica mold in UV-NIL, in which this hybrid materials by the combination of inorganic and organic components are interesting substances for their potentially increasing performance, such as elevated sensitivity, optical transparency, high density, high modulus and low dielectric constant.[18-27] Guo *et*

*al.* [19] developed a UV-curable formulation based on polysialic and polydimethylsiloxane to overcome some of the aforementioned shortcomings, such as a required inert atmosphere for its processing due to oxygen inhibition, high adhesion to the mold and so on. Willson, *et. al.*, introduced a bi-functional POSS with photosensitive acrylate and thermally curable benzoyl (BCB) groups to obtain ideal imprintable characteristics for UV-NIL. [20] They also reported POSS azide and POSS thiol for imprintable dielectric materials in UV-NIL.[21] Based on POSS thiol, Yin *et al.* focused on the click-reaction to get a high-resolution nanopattern in UV-NIL.[22,23] Meanwhile, Lee *et al.* used methacrylate multi-functionalized silsesquioxane (SSQMA) as key materials to prepare a nonstick replica mold with versatile functionality for mold-based, high-resolution nanolithography.[24,25] Although such kind of materials presents high reliability for patterning nano-structures, it still faces some challenges, such as compatibility, stability and high cost.

In this study, we aim to present a new kind of fluorinated silsesquioxane-based photoresist with various desirable characteristics for UV-NIL by incorporating fluorinated monomer of 1H,1H,7H-dodecafluorinatedheptyl methacrylate (FA) into octamethacrylated POSS (MA-POSS). Owing to its easy availability, low viscosity and low surface energy compared to other type of reactive monomer/oligomer materials, fluorinated surfactant is identified as a beneficial additive to optimize the overall performance of hybrid photoresist. Here we focus on the effect of photoresist's components including MA-POSS and FA on the curing rate, surface energy, viscosity, thermal stability and mechanical performance. With the optimized formulations for UV-NIL resists, a high-resolution pattern could be obtained with its special dimension range from dozens of nanometers to hundreds nanometers. These hybrid photoresist systems

with high performance are believed to have a great potential for inexpensive and convenient components in UV-NIL processes.

## 2 Experimental

### 2.1 Materials

3-methacryloxy propyl trimethoxyl silane (KH570) was provided from Anhui silicon Baoxiangfei Organic Silicon New Material Co., Ltd. 1H, 1H, 7H-Dodecafluorinatedheptyl methacrylate (FA) was purchased from Harbin Xuejia Chemical Co., Ltd. 1, 6-Hexamethylene diacrylate (HDDA) was provided by Sartomer Co., Ltd. The photoinitiator Darocure 1173 was obtained from Tronly (Changzhou, China) Co., Ltd. Isopropanol (IPA) and 25% aqueous solution of Tetramethylammonium hydroxide pentahydrate (TMAH) were purchased from Beijing Chemical Reagent Company.

### 2.2 Synthesis of MAPOSS

Synthesis of MA-POSS was similar with the previous report by H. Saito, [28] and the preparation process was further optimized in this study. 40 mL isopropanol solution including KH570 (38.07 g) was slowly dropped into 120 mL 25% aqueous isopropanol solution including 2.0 g TMAH for 30 min slow stirring. Then the mixture was stirred at room temperature for 2 hours. The solvent was removed through vacuum filtration to obtain colorless viscous liquid. To achieve neutral solution, the crude product solution was dissolved in toluene and then washed with saturated NaCl solution. The toluene phase was dried with anhydrous $MgSO_4$ and concentrated to obtain gummy liquid (20.64 g). The hydrolytic recondensation of the resulting product with 10% aqueous solution of TMAH (2.0 g) in toluene (100 mL) was carried out for six hours at 130 °C. After a serial of processes including concentration, washing and drying, the functionalized viscous

silsesquioxane (18.07 g) was obtained, which could be dissolved in most polar organic solvents, acrylate and methacrylate monomers and aromatic and aliphatic resins.

### 2.3 Nanoimprinting

A Nanonex 2000 imprinting tool (Monmouth Junction, NJ, USA) with vacuum capability and wavelength for UV curing at 365 nm or a light curing system (ELC-430) from Electro-Lite Corporation (Bethel, Ct, USA) was used for UV-NIL. The imprinting pressure was typically 300 psi. The silica substrate was washed by $H_2SO_4/H_2O_2$ with a weigh ratio (1:1) for 15 min and then treated with $O_2$ plasma. The selected photoresist was dispensed as a droplet onto the modified substrates, and then coated as the transfer film at 1,000 rpm for 40 s and 3,000 rpm for 20 s. After a baking process, the thickness of the obtained film was measured to be about 600 nm. Then the imprinting process was performed under UV light for 40 s at room temperature. Finally, $SiO_2$ or Polyethylene terephthalate (PET) mold was removed without other treatment. The detailed nanoimprinting process was demonstrated in Fig.1.

**<Figure 1>**

### 2.4 Measurements

$^{1}H$ NMR and $^{29}Si$ NMR spectra were recorded through an AV-600 NMR spectrometer (600 MHz) with $CDCl_3$ as the solvent. Chemical shifts are recorded in ppm from TMS with the residual protonated solvent as an internal standard ($CDCl_3$, 1H 7.24 ppm). FT-IR spectra were recorded on a Perkin–Elmer Paragon 1000. Gel permeation chromatography (GPC) measurements in THF were performed using a Waters515-241GPC system. The GPC was calibrated with monodisperse poly-(methyl methacrylate) (PMMA) standards with PDIs<1.04. X-ray diffraction patterns of the fabrics (XRD) were measured with a

D/max-2500 PC X-ray Diffractometer (Rigaku Corporation, Japan) under the operating conditions: Cu-K target at 40 kV 200 mA, k = 1.541 Å. Scanning electron microscopy (SEM) (Hitachi SU8000) and atomic force microscopy (AFM) (Veeco NanoMan) were used to characterize the surface morphologies of nanopatterns by UV nanoimprinting on glass and PET substrates.

The viscosities of the formulations were measured with a Anton Paar Phsica MCR301 (Anton Paar Gmbh, Austria) under rotational speed from 5 rpm to 100 rpm at 25 $^{o}$C. The kinetic parameters of the photopolymerization were determined by real-time Fourier transform infrared (FTIR) spectroscopy and Thermo-Nicolet 5700 instrument. The sample was exposed simultaneously to the UV beam to induce the polymerization for IR beam analysis. After the methacrylic group conversion, the absorbance decrease of the band centered at 6130 $cm^{-1}$ was monitored with the glass background. Based on the standard testing method ASTM D2765-84, the gel content was determined on the cured films by measuring the weight loss after 24-h's extraction with chloroform at room temperature. According to ISO 3521, a pycnometer was used to measure the density (ρ) of resists before and after curing. The bulk volumetric shrinkage was calculated by the formula:

$$Shrinkage\,\Delta V\% = \left(1 - \frac{\rho_{before}}{\rho_{after}}\right) \times 100\% \quad (1)$$

.

Thermogravimeatric analysis (TGA) was performed on a TGAQ50 at a heating rate of 10 $^{o}$C/min under $N_2$. The Young's moduli and hardness of coated resins were measured at room temperature with a commercial nanoindentation system (Nanoindenter XP; MTS Nano Instruments, Oak Ridge, TN). Contact angles between the surfaces and selected

liquids provided the information for calculating surface energies. With distilled and deionized water as the reference liquid, Contact angles were determined using a Dataphysics OCA 20 contact angle meter. The static contact angles of deionized water, diiodomethane, and glycol on the imprinted films were measured at ambient temperature. Static and sessile drops (10 μL) were delivered from a micrometer syringe with a minimum division of 2 μL. About 5 independent measurements were carried out and their average contact angle was recorded. The surface energy of the low-surface-energy materials based on the measured contact angles is calculated according to the van Oss–Good–Chaudhury (VOGC) equation of the Lewis Acid-Base Interaction Model:

$$2(\sqrt{\gamma_S^{LW}\gamma_L^{LW}} + \sqrt{\gamma_S^{+}\gamma_L^{-}} + \sqrt{\gamma_S^{-}\gamma_L^{+}}) = \gamma_L \times (1+\cos\theta) \quad (2)$$

Where, $\gamma^{LW}$ is the Lifshitz vander Waals component; $\gamma^{+}$ is the polar electron-acceptor (Lewis acid) component; $\gamma^{-}$ is the polar electron-donor (Lewis base) component. To get the three unknown values (i.e., $\gamma^{LW}$ ,$\gamma^{+}$ and $\gamma^{-}$), three liquids of known components can be used in the process of contact angle measurements, which will result in three equations and they can then be solved by the bulit-in command of MATLAB. The three common liquids used in contact angle measurements and their surface free energy parameters are shown in ESI (Table S1).

**Results and Discussions**

**Preparation and characterization of hybrid photoresists**

Herein, the MAPOSS was synthesized from a commercial organotrialkoxysilane with methacrylate groups by three steps. Firstly, as shown in Fig. 2a, the hydrolysis of alkoxy groups and the partial condensation of the resulting SiOH groups generated functional

group-containing hydrolysis products with the aid of the alkalic catalyst; and then the functionalized silsesquioxane was obtained from the hydrolytic recondensation with an alkaline catalyst. As shown in Fig. 3a, a remarkable peak related to Si-O-Si at 1099 $cm^{-1}$ was observed and the peak of $Si-OCH_3$ at 1162 $cm^{-1}$ or the peak of the $Si-CH_2$ at 1080 $cm^{-1}$ was not observed, indicating that the silicon cage hydrolysis reaction was completed. The peaks of C=C at 1640 $cm^{-1}$ and C=O at 1718 $cm^{-1}$ showed little change of the reactant (KH570), meaning that the functional methacrylate side chain was not involved in the reaction. It could be seen from $^{1}H$ NMR spectra in Fig. 3b that each peak can be assigned to the related proton of methacrylated-POSS. The ratio of proton remained the same as the reagent. The $^{29}Si$ NMR spectrum shows the $T^3$ signal of the cage structure where the split was between 65 and 75 ppm (Fig. S1). Other characterization data were also provided in ESI (Figs. S2 and S3). All of these results demonstrate that the MAPOSS was successfully synthesized.

For the UV-NIL, it's desirable that the photoresists should have the properties of low viscosity, high curing efficiency and low surface energy.[3,6] The structures of the different components in our hybrid photoresist are shown in Fig. 2b. As one of the main ingredients of the hybrid photoresists, 1H,1H,7H-dodecafluorinatedheptyl methacrylate (FA) is an reactive diluent fluorinated monomer to reduce viscosity. More importantly, it is an ideal agent of low surface energy, which was useful in demolding as mentioned in previous study.[17] 1, 6-hexamethylene diacrylate (HDDA) was selected as the crosslinker for its elevated crosslinking density and high flexibility. The MAPOSS was adopted as the oligomer to provide accelerated cured rate and high mechanical properties as mentioned above. Darocure 1173 was used as a photoinitiator for radical photopolymerization in all the photopolymer films.

**<Figure 2>**

**<Figure 3>**

**Viscosity and surface properties of hybrid photoresists**

In order to get the optimal photoresist components, a series of hybrid resists were prepared by changing the mass ratio between MAPOSS and FA, as shown in Table 1. The prepared resists are the transparent and homogeneous oil with good compatibility and stability. As for the UV-curable resist, low viscosity plays a decisive role for high efficiency and accuracy of UV-NIL, we found that by incorporating the low viscous acrylic reactive diluents, the viscosities of the resins were drastically reduced from 1700 cP to the value between 5.5 and 60.1 cP. Additionally, the viscosity was decreased with the decreasing content of MAPOSS as listed in Table 1, indicating that MAPOSS content had a direct effect on the viscosity.

**<Table 1>**

All photopolymerization films were prepared by the following procedure. The UV curable resist were spin coated onto silica substrates after a series of surface treatments as mentioned in experimental section. The thin films were then cured by exposure to 365 nm UV light at an intensity of 10 $mW/cm^2$ for appropriate time under a nitrogen atmosphere. Due to Van der Waals' forces, polymerization shrinkage of photoresist occurred when the distance between monomers changed within the distance of covalent bonds of the resultant polymers upon light curing. As listed in Table 1, the bulk shrinkage was remarkably reduced by adding the MAPOSS into the polymer according to the ratio from 2.8% to 9.1%, which was much lower than that of the conventional methacrylate resists (~11%). This may be attributed to the rigidity and steric hindrance of the functional

groups. For the bulky MAPOSS with eight methacrylate arms, MAPOSS could not approach each other freely and the cross-linked hybrid provides an anchor point within a polymer matrix.

Additionally, contact angles between the surfaces and three selected liquids provide the information on surface energies according to the van Oss–Good–Chaudhury (VOGC) Equation. As summarized in Table 1, surface energy was obviously decreased with the increasing content of fluorinated monomer (FA), which implies that the addition of FA can lower the surface energy of the cured hybrid resist. When the mass content was above 35%, the cured film showed desirable surface and interface properties for easier release. Based on the above analysis, we think our hybrid resists have the potential to be used as photoresist for UV-NIL due to their low viscosity, low shrinkage and low surface energy.

**Photopolymerization kinetics of hybrid photoresists**

Kinetic curing profiles of UV photoresist were investigated by a Real Time FTIR, it was found that tracing induction and conversion period of acrylic double bond were greatly affected by oligomer, photo-initiators and acrylic monomers as well as irradiance and spectrum. To simulate the imprint scene, glass was used as the background. The dose was launched at 5.96 s to make a comparison between the fresh and the cured resins. FTIR spectra of –C=C– exposed for various reaction time was shown in Fig. 4, in which the peaks at 6130 $cm^{-1}$ is attributed to –C=C–. It is obvious that the increasing FA content in the photocurable formulation induces a slightly decrease of photopolymerization rate. Nevertheless, when the curing is completed, the absorption peak intensity basically has no change. The curing rates and conversion are closely related to the MAPOSS content in weight. The addition of the MAPOSS can accelerate the reaction rate, and increase the curing efficiency. However, too high content of –C=C– is not conducive to improve the

conversion rate. And the resist with a lower mole ratio of MAPOSS/FA can reach 93% conversion rate.

**<Figure 4>**

**Mechanical properties and thermal stability of hybrid photoresists**

The performance in feature integrity and transfer efficiency related to the mechanical properties is a key evaluation indicator for NIL.[6] Rigid materials with tensile modulus above 100 MPa, are appropriate for reproducible replication with little feature collapse at the 50 nm scale. The moduli and hardness of the fully cured formulations were investigated with nanoindentation technique. Fig. 5 shows that the Young's modulus and hardness of the cured resists are function of the contact depth. The mechanical properties are uniform and stable between 30 and 400 nm. The Young's modulus of curing formulation is increased with the content of MAPOSS. The results show that the MAPOSS can enhance the mechanical property efficiently. The modulus of the sample with 13.4 wt% MAPOSS is 2.85 GPa, which is rigid enough for building the nanostructured patterns to resist failures for NIL.

Thermal gravimetric analysis in Fig. 6 shows that the hybrid resists exhibit better thermal stability than the pure organic polymer. Resists with higher MAPOSS content exhibits higher thermal weight loss temperature at 5% mass loss, which is due to that the MAPOSS is conducive to increase crosslinking density of the organic matrix during the photopolymerization. These results also suggest a homogeneous phase of the cured polymer and the cage structure of MAPOSS can efficiently enhance the heat resistance.

**<Figure 5>**

**<Figure 6>**

**Nanopatterns of UV Nanoimprinting**

To verify the applicability of the fluorinated silsesquioxane-based photoresist in the UV-NIL process, patterning of the photoresist with MAPOSS/FA=0.25 was performed on glass substrates as shown in Fig. 1, two hard $SiO_2$ molds with feature sizes of several hundreds nanometers were used to verify the ability of the photoresist of MAPOSS/FA=0.25 to form nanostructures. As shown in SEM images of Fig. 7a and 7c, the photoresist of MAPOSS/FA=0.25 with low viscosity were successfully duplicated from the $SiO_2$ master to the nanostructures using UV irradiation at 25 $^oC$ and low pressure over a relatively short period of time (40 s). Most importantly, almost no signs of defects were observed from the magnification images in Fig. 7b and 7d, respectively. These results demonstrate good coating properties and low surface energy of the hybrid resists allow them to be easily released from molds and obtain high-quality patterns during the demolding process.

Additionally, we evaluate the patterning of fluorinated silsesquioxane-based photoresist on a flexible PET substrate, Fig. 8a shows that real image of the patterns on PET, and the corresponding SEM and AFM images of the imprinted grating with 140 nm line widths were exhibited in Fig. 8b-d, respectively. It is obviously seen that fluorinated silsesquioxane-based photoresist can be easily patterned on top of a flexible substrate with a high quality. Additionally, even if a mold with a higher resolution was used, the imprinted nanopattern was also obtained with good feature as shown in Fig 8e and 8f. Here the patterning area is just limited by the availability of the mold and the dimension of the curing light sources. In fact, we think this kind of hybrid photoresist is also suitable for continuous roll-to roll nanoimprinting. We also note that the patterns obtained from

fluorinated silsesquioxane-based photoresist on PET substrate can be used as a flexible and easily replicable mold to replace the original $SiO_2$ or Si mold.[19]

**<Figure 7>**

**<Figure 8>**

## Conclusions

To summarize, a new kind of fluorinated silsesquioxane-based photoresist has been developed for ultraviolet nanoimprint lithography (UV-NIL). A facile synthesis route is firstly presented for octamethacrylated polyhedral oligomeric silsesquioxane (MAPOSS). Then the hybrid photoresists composed of MAPOSS, fluorinated monomer and crosslinker were fabricated which exhibited desirable characteristics for UV-NIL application, such as high curing rate, low surface energy, low viscosity (5.9–60.1 cP) and low bulk volumetric shrinkage (6.14%), together with increased thermal stability (342-352 $^{o}$C) and high Young's modulus (2.84–3.13 GPa). With the optimized formulations for UV-NIL resists, a high-resolution pattern could be achieved with its special dimension in the range from dozens of nanometers to several nanometers both on the glass and flexible substrates. This work shows the potential to use simple but multifunctional hybrid components of photoresists for future UV-NIL applications.

## Acknowledgement

This work was supported by Beijing Municipal Natural Science Foundation (Grant No. 2102035), National Natural Science Foundation of China (Grant No. 51173013 and 51373013) and Beijing Young Talents Plan (YETP0489). We are grateful to Prof. L. Jay

Guo, Dr. Tao Ling and Mr. Cheng Zhang of Department of Electrical Engineering and Computer Science of University of Michigan for their help of nanoimprinting experiment and related discussion.

**References**

1 S. Y. Chou, P. R. Krauss and P. J. Renstrom, *Appl. Phys. Lett.*, 1995, **67**, 3114.

2 X. Liang, K. J. Morton, R. H. Austin and S. Y. Chou, *Nano. Lett.*, 2007, **7**, 3774.

3 L. J. Guo, *Adv. Mater.*, 2007, **19**, 495.

4 D.-H. Ko, J. R. Tumbleston, L. Zhang, S. Williams, J. M. DeSimone, R. Lopez and E. T. Samulski, *Nano. Lett.*, 2009, **9**, 2742.

5 X. Cheng, L. J. Guo and P. F. Fu, *Adv. Mater.*, 2005, **17**, 1419.

6 H. Schift, *J. Vac. Sci. Technol. B*, 2008, **26**, 458.

7 P. Wang, J. Guo, H. Wang, Y. Zhang and J. Wei, *J. Phys. Chem. C*, 2009, **113**, 8118.

8 A. E. Hollowell and L. J. Guo, *Adv. Optical Mater.*, 2013, **1**, 343.

9 Y. J. Shin, Y. K. Wu, K.-T. Lee, J. G. Ok and L. J. Guo, *Adv. Optical Mater.*, 2013, **1**, 863.

10 H. J. Park, T. Xu, J. Y. Lee, A. Ledbetter and L. J. Guo., *ACS Nano*, 2010, **4**, 4776.

11 B. D. Lucas, J.-S. Kim, C. Chin and L. J. Guo, *Adv. Mater.*, 2008, **20**, 1129

12 H.-G. Park,a J.-J. Lee, K.-Y. Dong, B.-Y. Oh, Y.-H. Kim, H.-Y. Jeong, B.-K. Ju and D.-S. Seo, *Soft. Matter.*, 2011, **7**, 5610

13 H. Lan and H. Liu, *J. Nanosci. Nanotechnol.*, 2013, **13**, 3145.

14 M. Fukuhara, H. Ono, T. Hirasawa, M. Otaguchi, N. Sakai, J. Mizuno and S. Shoji, *J. Photopoly. Sci. Technol.*, 2007, **20**, 549

15 B. K. Long, B. K. Keitz and C. G. Willson, *J. Mater. Chem.*, 2007, **17**, 3575.

16 K.-S. Kim, J.-H. Kim, H.-J. Lee and S.-R. Lee, *J. Mater. Sci. Technol.*, 2010, **24**, 5.

17 S. Ito, C. M. Yun, K. Kobayashi and M. Nakagawa, *J. Vac. Sci. Technol.B*, 2012, **30**, 06FB05.

18 H. W. Ro, V. Popova, L. Chen, A. M. Forster, Y. Ding, K. J. Alvine, D. J. Krug , R. M. Laine and C. L. Soles, *Adv. Mater.*, 2011, **23**, 414

19 C. Pina-Hernandez, L. J. Guo and P.-F. Fu, *ACS Nano*, 2010, **4**, 4776.

20 J. Hao, M. W. Lin, F. Palmieri, Y. Nishimura, H.-L. Chao, M. D. Stewart, A. Collins, K. Jen and C. G. Willson, *Proc. SPIE*, 2007, 6517.

21 C. G. Wilson, *J. Photopolym. Sci. Technol.*, 2009, **22**, 147.

22 H. Lin, X. Wan, X. Jiang, Q. Wang and J. Yin, *Adv. Funct. Mater.*, 2011, **21**, 2960.

23 H. Lin, X. Wan, X. Jiang, Q. Wang and J. Yin, *J. Mater. Chem.*, 2012, **22**, 2616.

24 B. K. Lee, N.-G. Cha, L.-Y. Hong, D.-P. Kim, H. Tanaka, H. Y. Lee and T. Kawai, *Langmuir*, 2010, **26**, 14915.

25 B. K. Lee, H. Cho and B. H. Chung, *Adv. Funct. Mater.*, 2011, **21**, 3681.

26 B. K. Lee, T. Kawai and B. H. Chung, *Macromol. Biosci.*, 2011, **11**, 600.

27 B. K. Lee, K.-S. Park, D.-P. Kim, J.-H. Ryu, J. Park, Y.-S. Jeong, K.-H. Baek and L.-M. Do, *J. Mater. Chem.*, 2012, **22**, 16754.

28 H. Saito and M. Isozaki, JP285387, 31[P], 2002.

**Figure captions**

**Table 1:** The components and some physical properties of the hybrid resists. The weight of the photoinitiator 1173 is 4 wt% as the crosslinker is 30 wt% in the whole resist.

**Figure 1:** Schematic illustration of UV-NIL process and the corresponding photoresist materials.

**Figure 2:** Synthesis of MAPOSS and chemical structure of each component of the hybrid UV-NIL resist.

**Figure 3:** (a) FT-IR spectra of the MAPOSS and the KH570 and (b) $^{1}H$ NMR spectra of MAPOSS in $CDCl_3$.

**Figure 4:** Conversion and curing rate (differential curve) of various fluorinated silsesquioxane-based photoresists.

**Figure 5:** The hardness (a) and Young's modulus (b) as a function of the contact depth of various fluorinated silsesquioxane-based photoresist.

**Figure 6:** TGA curves of the fluorinated silsesquioxane-based photoresist.

**Figure 7**: (a) and (c): SEM images of the imprinted pattern by fluorinated silsesquioxane-based photoresist on glass substrate; (b) and (d): the corresponding magnification SEM images, respectively.

**Figure 8:** (a) Fluorinated silsesquioxane-based photoresist patterned on a flexible PET substrate; (b) SEM image of the imprinted grating with 140 nm line width; (c) and (d): the corresponding AFM images of the patterns with 140 nm line width; (e) and (f) SEM images of around 50 nm size dense rod structures patterned on a PET substrate.

Table 1. The components and some physical properties of the hybrid resists. The weight of the photoinitiator 1173 is 4 wt% as the crosslinker is 30 wt% in the whole resist.

| Resist | F content(wt%) | Mole ratio of MAPOSS/FA | Viscosity (cP) | Surface energy ($mJ/m^2$) | Shrinkage (%) | Hard (MPa) | Young's modulus (GPa) |
|---|---|---|---|---|---|---|---|
| FMH1 | 10 | 0.77 | 60.11 | 34.8 | 2.80 | 220 | 3.13 |
| FMH2 | 20 | 0.25 | 27.16 | 32.1 | 5.41 | 197 | 2.96 |
| FMH3 | 30 | 0.07 | 16.94 | 22.9 | 6.14 | 156 | 2.85 |
| FMH4 | 35 | 0.02 | 5.86 | 20.1 | 9.12 | 142 | 2.84 |

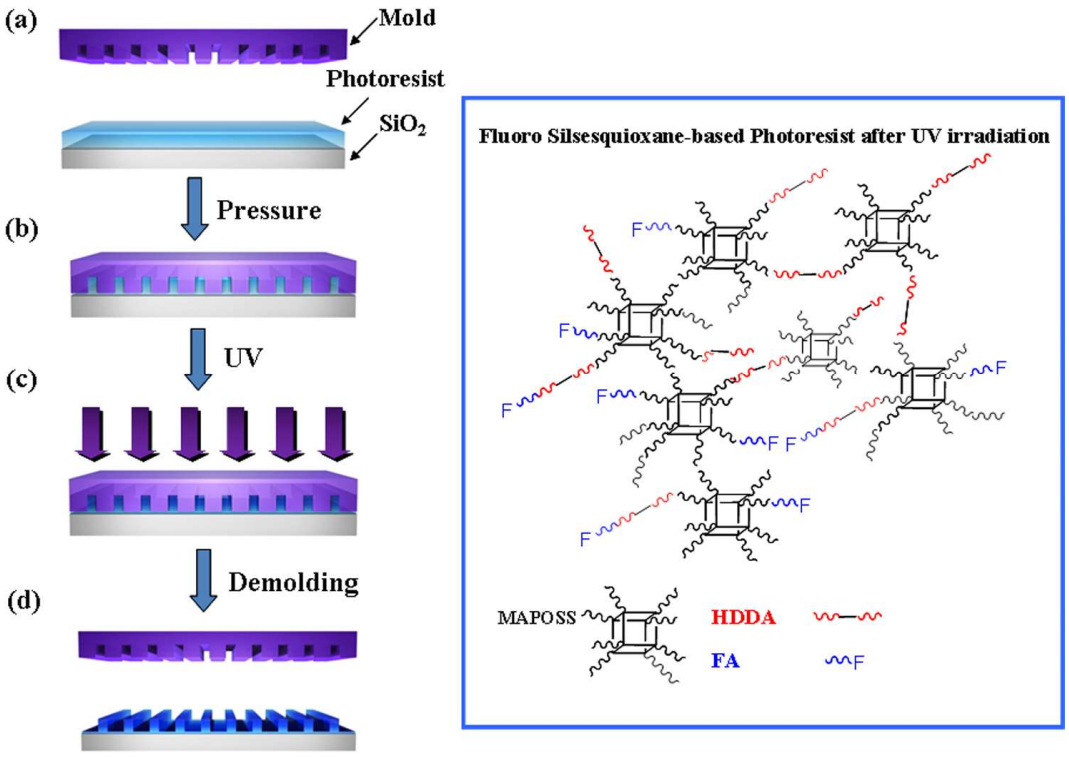


**Figure 1**

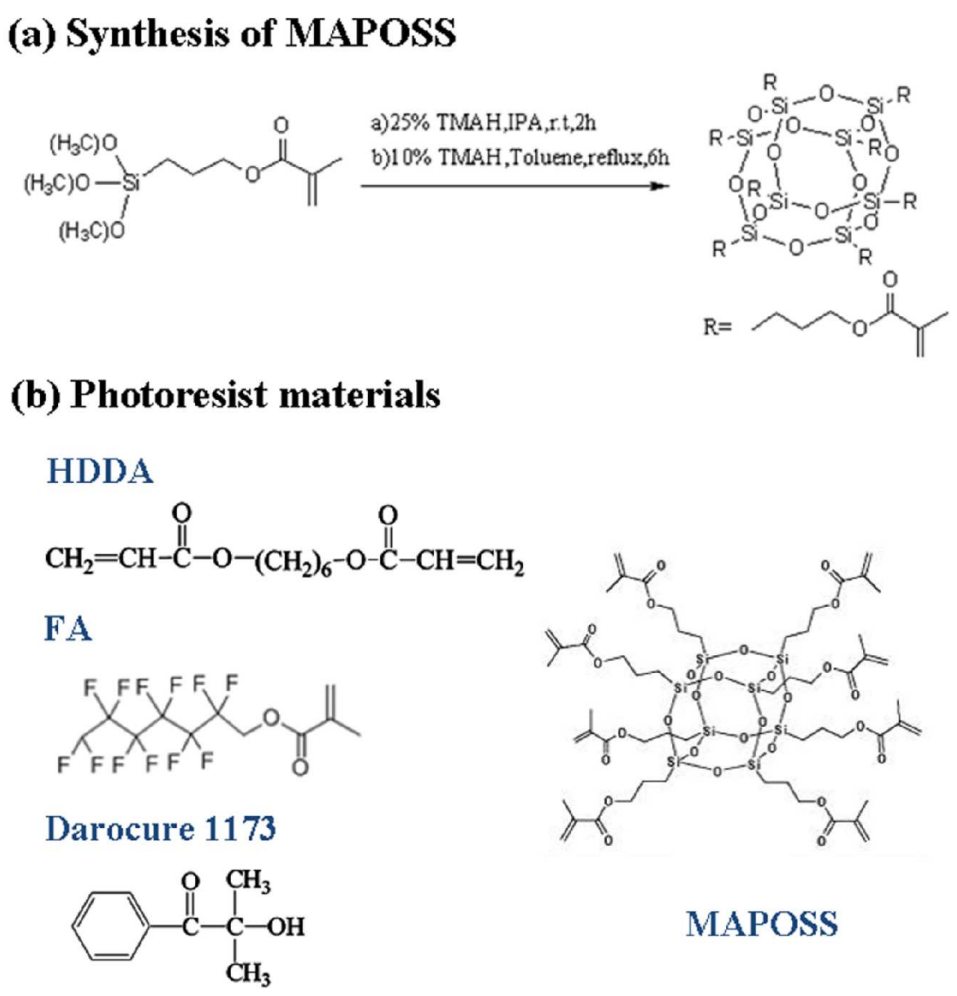


**Figure 2**

**(a)**

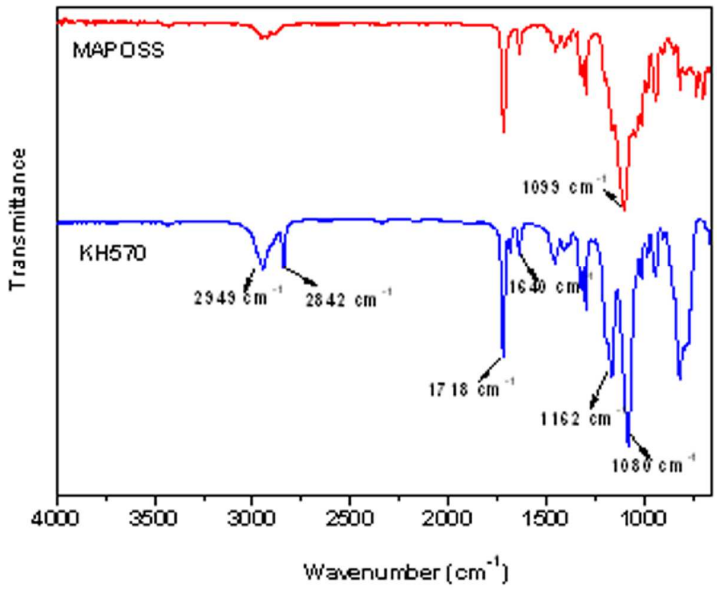


**(b)**

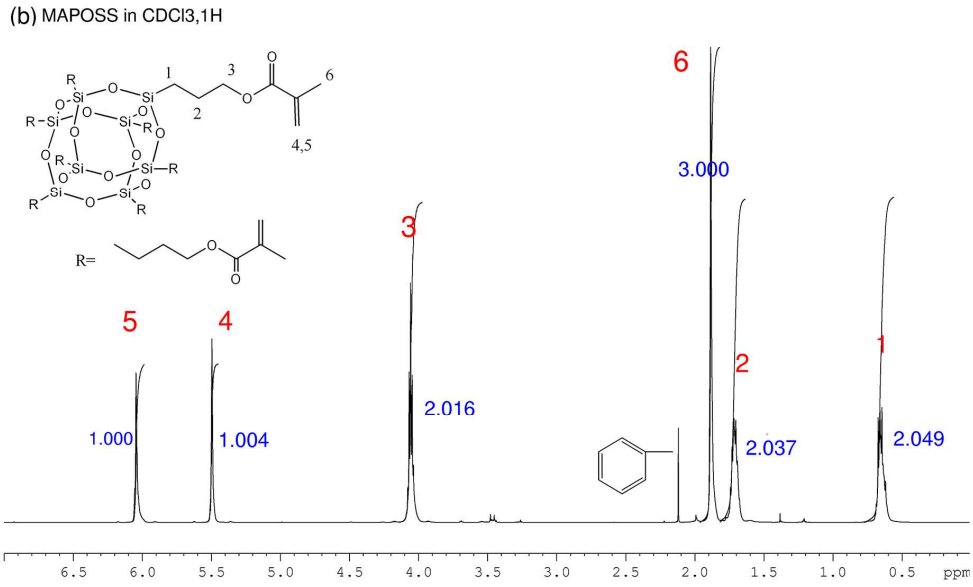


**Figure 3**

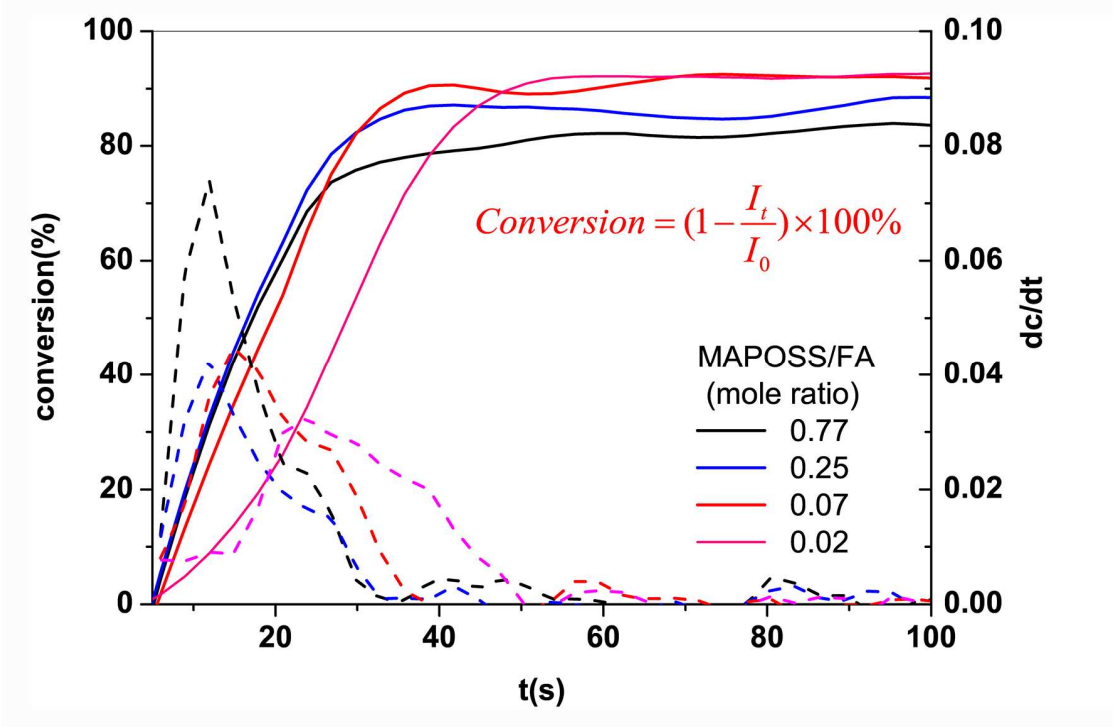


**Figure 4**

(a)

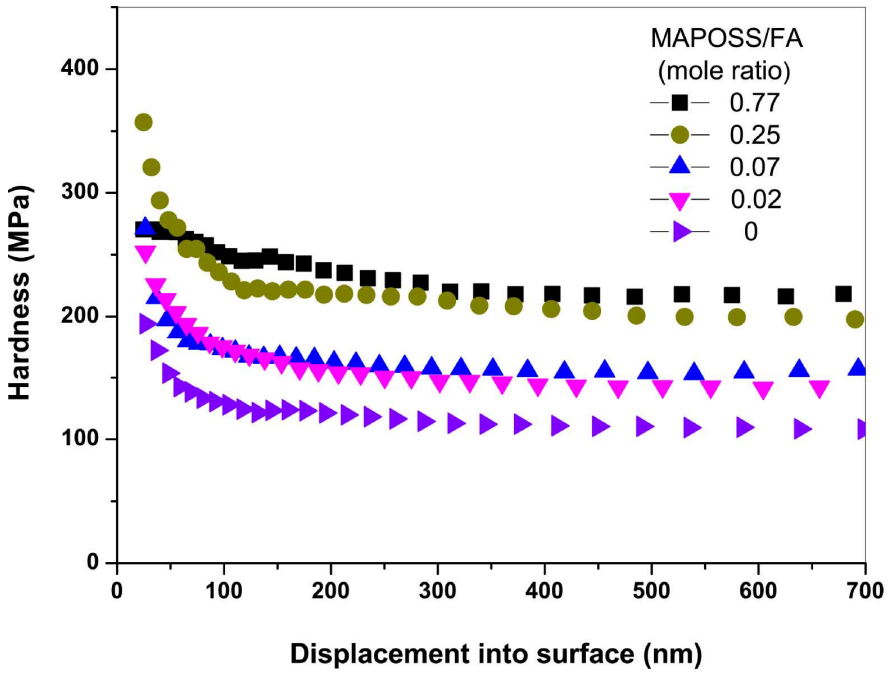


(b)

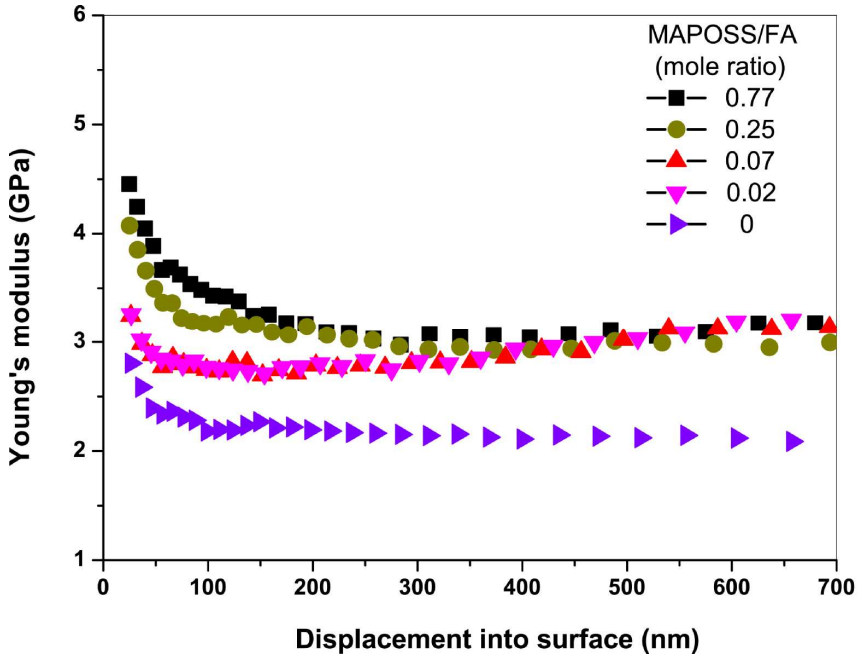


Figure 5

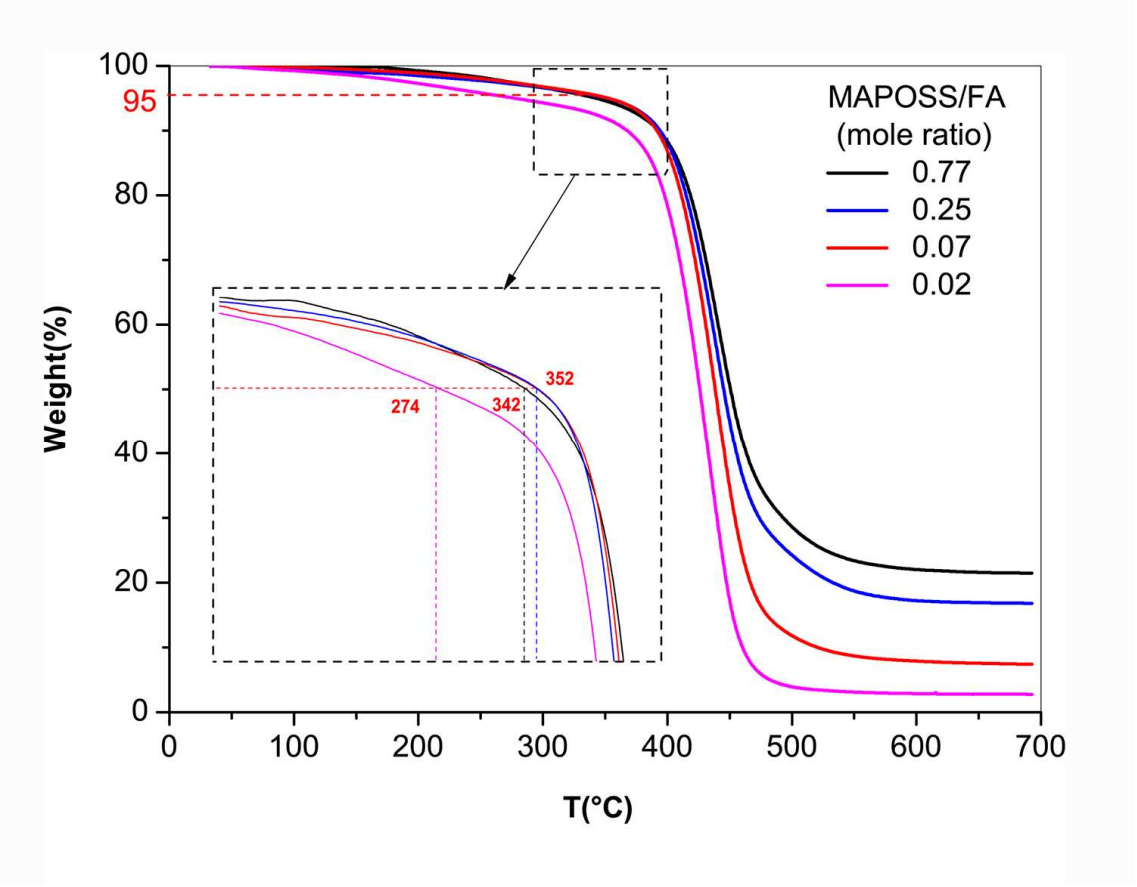


**Figure 6**

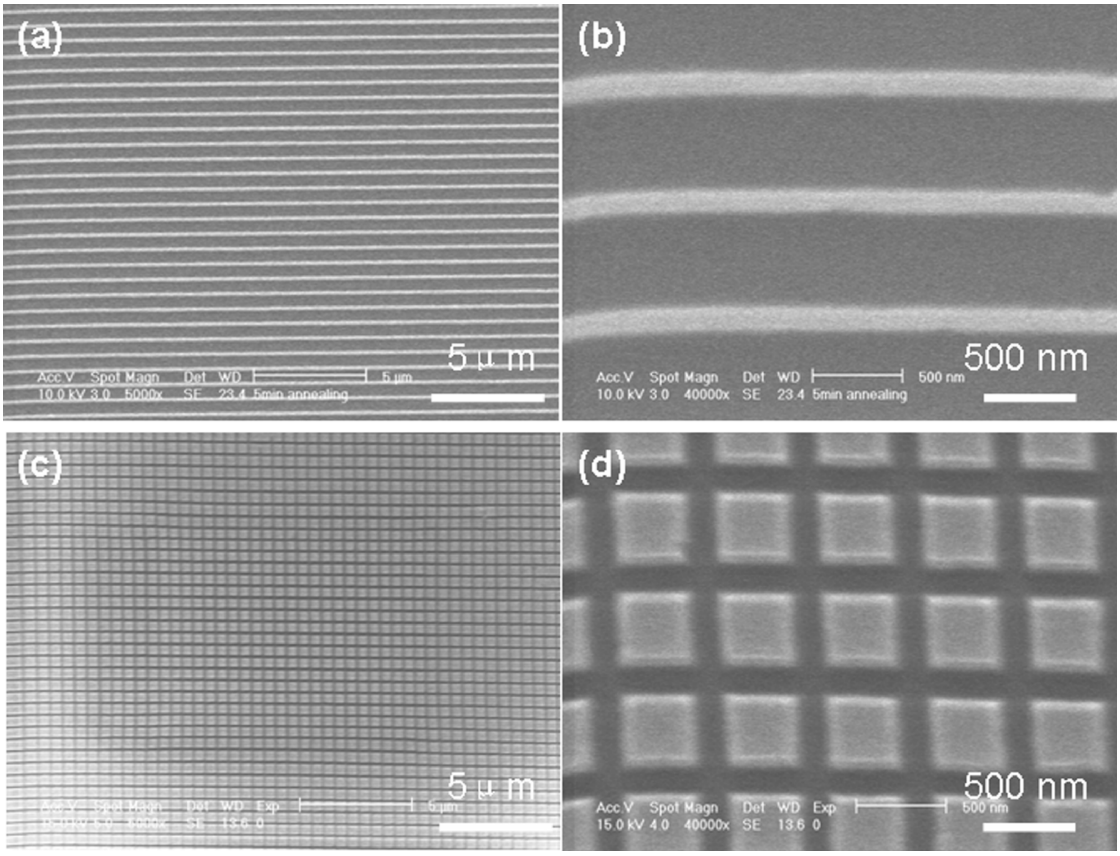


**Figure 7**

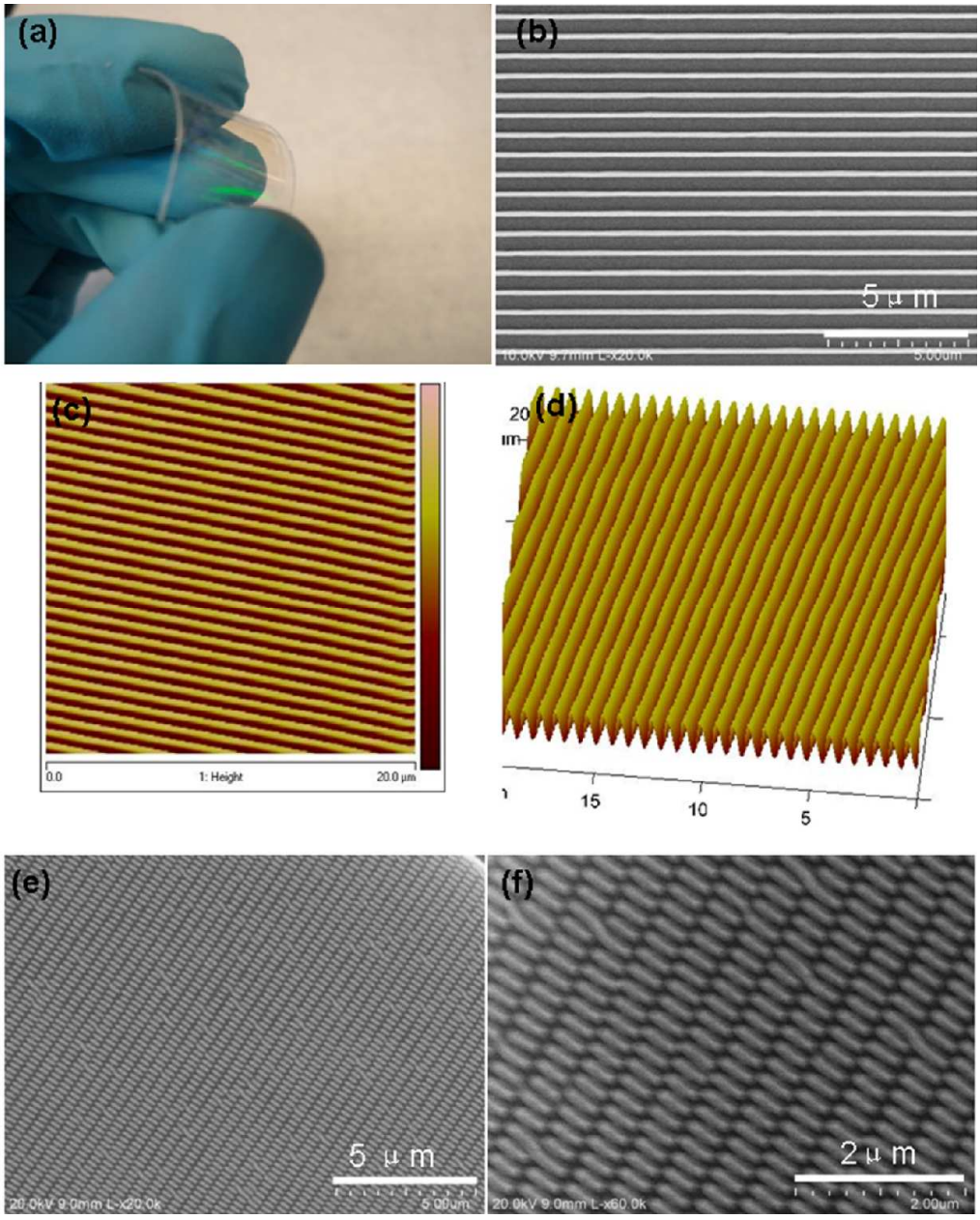


**Figure 8**

Graphic Abstract:

# Table of contents entry

**Text:**

A new kind of fluorinated silsesquioxane-based photoresist has been demonstrated for ultraviolet nanoimprint lithography (UV-NIL). We believe that this work opens up a way to utilize simple but multi-functional components materials for developing photoresist with superior performance for the practical UV-NIL application.

**Color graphic:**